Beta Spectrum of Cl^{36}†

R. G. JOHNSON, O. E. JOHNSON, AND L. M. LANGER
Department of Physics, Indiana University, Bloomington, Indiana

(Received February 13, 1956)

The twice forbidden beta spectrum of Cl^{36} has been measured with a 4π scintillation spectrometer which is particularly well suited for measuring beta spectrum shapes from sources with low specific activity. The distribution was measured to as low as 89 kev with three sources of average thicknesses of 9, 19, and 20 $\mu g/cm^2$. The data were analyzed by using the exact twice forbidden shape factor for the linear combination of the S and T couplings for $\Delta J=2$. The ratios of nuclear beta moments appearing in the shape factor were treated as variable parameters. The best fit to the data was for $R_{ij}/T_{ij}=0$ and $A_{ij}/T_{ij}=14.2$.

INTRODUCTION

THE beta spectrum of the twice forbidden decay of Cl^{36} has been studied with very thin sources by means of a scintillation spectrometer employing 4π solid angle geometry. The data have been used to evaluate the ratios of nuclear β moments (matrix elements) that occur for a linear combination of the scalar and tensor forms of the interaction.

Previous measurements[1,2] do not agree on the shape of the spectrum in the low-energy region. The proportional counter measurements of Fulbright and Milton[2] show relatively fewer low-energy electrons than do the magnetic lens spectrometer measurements of Wu and Feldman.[1] These data were analyzed using a low-Z approximation of the twice forbidden shape factor, C_{2T},[3] for the pure Tensor interaction. Using the ratio of β moments, which appear in C_{2T}, as a parameter, Wu and Feldman found agreement for $A_{ij}/T_{ij}=4.2$. A similar analysis of the proportional counter data by Fulbright and Milton gave $A_{ij}/T_{ij}=5.1$.

The present investigation of the Cl^{36} spectrum was made to determine the shape of the spectrum at low energies and to evaluate the ratios of nuclear β moments which appear in the "exact" twice forbidden shape factor for the linear combination of the scalar and tensor interactions. The spectrum was measured with a 4π scintillation spectrometer for three sources whose average thicknesses were 9, 19, and 20 $\mu g/cm^2$. A 5-cm^2 source area and the 4π source-detector geometry made it possible to obtain a large number of points on each spectrum with good counting statistics. Consistent results were obtained for the three different sources.

Cl^{36} decays with a half-life of 4.4×10^5 years[4] by a single transition to the ground state of A^{36}. The ground state spin of Cl^{36} has been determined experimentally[5] as two. A^{36}, an even-even nucleus, is presumed to have a ground-state spin of zero. The shell model predicts no change in parity. This, along with a logft of 13.5, classifies the transition as twice forbidden with a spin change of two.

The theoretical shape factor for a twice forbidden transition with a spin change of two depends on which interaction form or forms are assumed appropriate for the transition. Mahmoud and Konopinski[6] have shown that the scalar (S) and tensor (T) components are essential and that the existing experimental evidence indicates the absence of any appreciable amount of the vector (V) and pseudovector (A) components. Therefore, the "exact" shape factor that is used for the analysis of the present data is the one which results from a linear combination of the S and T components. The ratios of nuclear β moments which appear in the exact shape factor are treated as free parameters and varied to obtain the best fit to the present experimental results.

The data have also been analyzed by using the low-Z approximation of the exact shape factor and the low-Z approximation of the twice forbidden shape factor for the pure tensor interaction. These analyses are used to compare the present experimental results with those of other investigators and to check on the conclusions drawn from the analysis of the data with the exact shape factor. The low-Z approximation of the exact shape factor is also used for determining the end point of the spectrum which is then used in calculating the experimental shape factor.

EXPERIMENTAL APPARATUS

A beta spectrum measured with a scintillation spectrometer which uses only one scintillator as a detector and an external source is badly distorted in the low-energy region of the spectrum. Jordan and Bell[7] suggested that this effect was largely the result of scattering of the beta particles out of the scintillator. By sandwiching a beta-ray source between two anthracene crystals which were mounted on a photomultiplier tube, Ketelle[8] showed that Jordan and Bell's explanation of the distortion was correct. A 4π beta-ray

† Supported by the joint program of the Office of Naval Research and the U. S. Atomic Energy Commission and by a grant from the Research Corporation.

[1] C. S. Wu and L. Feldman, Phys. Rev. **76**, 693 (1949); **87**, 1091 (1952).
[2] H. W. Fulbright and J. C. Milton, Phys. Rev. **82**, 274 (1951).
[3] E. J. Konopinski, Revs. Modern Phys. **15**, 209 (1943).
[4] Wu, Townes, and Feldman, Phys. Rev. **76**, 692 (1949).
[5] C. H. Townes and L. C. Aamodt, Phys. Rev. **76**, 691 (1949).
[6] H. M. Mahmoud and E. J. Konopinski, Phys. Rev. **88**, 1266 (1952).
[7] W. H. Jordan and P. R. Bell, Nucleonics **5**, No. 10, 30 (1949).
[8] B. H. Ketelle, Phys. Rev. **80**, 758 (1950).

scintillation spectrometer which is capable of utilizing large source areas has been built in this laboratory. The 4π source-detector geometry is obtained by mounting the source between two plastic scintillators with a phototube viewing each scintillator (Fig. 1). For the present investigations, plastic scintillators 1.75 in. in diameter and 0.625 in. thick were optically coupled with silicon fluid to Dumont 6292 phototubes. Pulses from the phototubes go into preamplifiers whose output pulses are added in an electronic, linear addition circuit. Thus, an output pulse then corresponds to the full energy of a beta particle whether it is stopped in one scintillator or scattered from one into the other. The output pulses from the addition circuit are amplified further and then analyzed in a ten-channel differentia-discriminator. The pulse heights from the two photol tubes are matched by varying the high voltage on each tube separately. The high voltages are monitored and maintained to about $\pm 0.02\%$. Calibration of the spectrometer with internal conversion electrons of known energy usually preceded and followed each measurement of a beta spectrum. The percentage change in calibration pulse heights before and after runs which were as long as 9 hours was less than 2%. Figure 1 shows a block diagram of the experimental arrangement.

To determine the energy response of the plastic scintillator,[9] the pulse heights from internal conversion electrons of different energies have been measured. The internal conversion electrons were from the decay of Bi^{207} (976 kev), Cs^{137} (624 kev), In^{114} (162 kev), and Sn^{119m} (61 kev, L-line), Fig. 2 shows a plot of the results. The energy response of the plastic scintillator is linear from 61 kev to 976 kev but the linear extrapolation to zero pulse height intersects the energy axis at 10 kev. This is similar to the result found by Hopkins[10] for anthracene, for which the straight line intersected the energy axis at 20 kev.

As a further check of the reliability of the 4π beta-ray scintillation spectrometer, the beta spectra of P^{32}, Tl^{204}, and W^{185}, whose shapes are known from magnetic spectrometer measurements, have been investigated.

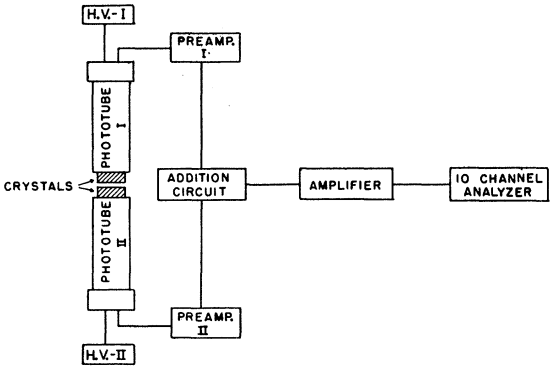

FIG. 1. Block diagram of apparatus.

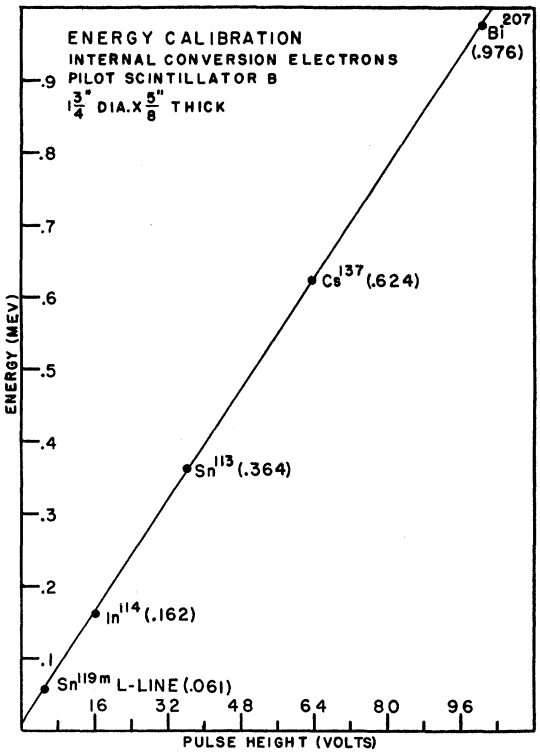

FIG. 2. Energy response of plastic phosphor.

Each of the sources was prepared in the following manner. A zapon film of less than 8 $\mu g/cm^2$ in thickness was placed over one of the scintillators. The source material was deposited from an aqueous solution on this film and was spread with the aid of insulin[11] over a circular area of about 5 cm^2 at the center of the scintillator. The other scintillator was covered by a zapon film of less than 8 $\mu g/cm^2$ and the two scintillators were brought into "contact" for the run. The average source thicknesses were less than 1 $\mu g/cm^2$ as determined from the Oak Ridge assays of the source materials and the total counting rates of the sources.

The P^{32} spectrum was measured with the ten-channel analyzer with 2% window widths. The full-width resolution of the spectrometer for this run was 12.9% for the 624-kev internal conversion line from the Cs^{137} decay. In the region below 1.1 Mev, at least 10^4 counts were taken at each point and below 1.6 Mev at least 10^3 counts were taken at each point. The background counting rate, which was less than 1% of the source counting rate except near the end point of the spectrum, was subtracted. A conventional Fermi-Kurie (F-K) plot of the data, before corrections for the finite resolution of the spectrometer were applied, is shown by the upper curve in Fig. 3. The effect of the resolution on

[9] Pilot Chemicals, Inc., 47 Felton Street, Waltham, Massachusetts.

[10] J. I. Hopkins, Phys. Rev. 77, 406 (1950).

[11] L. M. Langer, Rev. Sci. Instr. 20, 216 (1949).

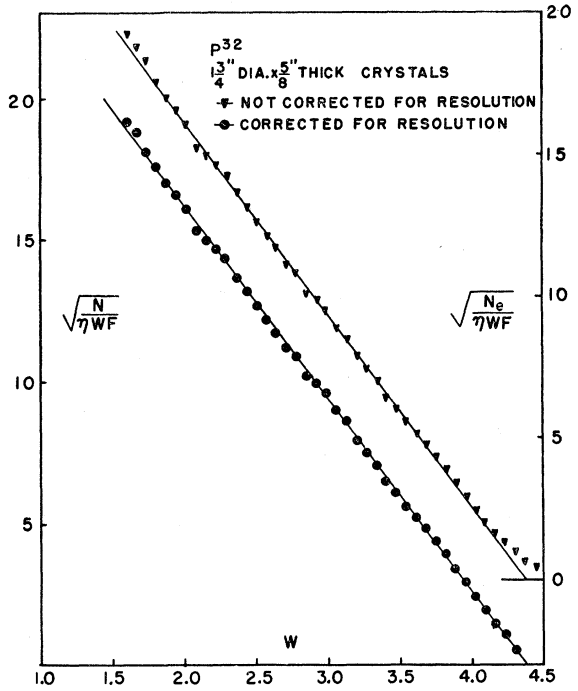

FIG. 3. P^{32} Fermi-Kurie plot with and without resolution corrections.

the shape of the spectrum near the end point is evident, but very little distortion is seen in the "body" of the spectrum. The lower curve in Fig. 3 shows the F-K plot after the resolution corrections of Palmer and Laslett[12]

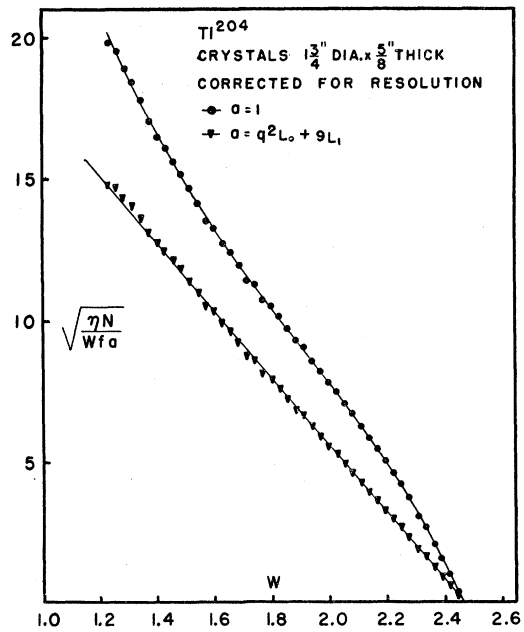

FIG. 4. Tl^{204} Fermi-Kurie plot.

[12] J. P. Palmer and L. J. Laslett, U. S. Atomic Energy Commission Bulletin ISC-174 (1950)

are applied. The resolution correction was less than one percent for any point on the spectrum except for the six points nearest the end point. The corrected F-K plot is in good agreement with the results of magnetic spectrometer measurements and the end-point energy of 1.72 Mev also agrees well. Calibration of the spectrometer for this run was made with the 976-kev internal conversion line from the decay of Bi^{207}.

The spectrum of Tl^{204} was obtained in a similar manner to that of P^{32}. The spectrometer was calibrated with the 624-kev internal conversion line from the Cs^{137} decay and the resolution of the spectrometer for this line was 11.6%. Corrections to the data for the resolution of the instrument were less than two percent at any point on the spectrum except for the six highest energy points. A conventional F-K plot of the data after resolution corrections were applied is shown by the upper curve in Fig. 4. This plot exhibits the characteristics of a beta spectrum with a unique once forbidden shape. The lower curve in Fig. 4 shows the F-K plot with the unique once-forbidden shape factor included. The end-point energy of 748 kev is in reasonable agreement with the values from the magnetic spectrometer measurements.

The beta spectrum of W^{185} was obtained in a similar manner to that of P^{32}. Calibration of the spectrometer was obtained from the 364-kev internal conversion line from the decay of Sn^{113}. The full-width resolution of the spectrometer was 12.0% for the 624-kev Cs^{137} line. Resolution corrections to the data were less than 2% at any point on the spectrum except for the nine highest energy points. A conventional F-K plot of the corrected spectrum is seen in Fig. 5. The plot is quite linear from the end point down to the 56 kev which was the lowest energy that could be measured without changing the pulse amplification for the spectrometer. The background counting rate was less than 5% of the source counting rate for points below 390 kev. The end-point energy of 434 kev is in good agreement with the values from the magnetic spectrometer measurements.

BETA SPECTRUM OF Cl^{36}

The present data from the Cl^{36} activity were obtained in essentially the same manner as the data from the activities already discussed. The calibration and resolution of the spectrometer were established from the 624-kev line from the Cs^{137} decay.

Five microcuries of Cl^{36} source material with a specific activity of 0.28 mC/g were obtained as HCl from the Oak Ridge National Laboratory where the activity was produced by the pile reactions $Cl^{35}(n,\gamma)Cl^{36}$. This material was transformed to NH_4Cl for use as a source.

The Cl^{36} beta spectrum was obtained from three different sources over a period of about one month. In each of the three runs, a water solution of NH_4Cl was spread with the aid of insulin over a 5-cm^2 disk at the center of a 7-$\mu g/cm^2$ zapon film and the two scintil-

lators placed in contact with the source sandwiched between them. (See Fig. 1.) The average source thicknesses were calculated on the basis of the total counting rate of the source and the total weight and activity of the source material as given by the Oak Ridge National Laboratory assay.

The first run on Cl^{36} was made with a 9-$\mu g/cm^2$ source whose total activity was 8 millimicrocuries. At least 6×10^3 counts were recorded for each point below 650 kev. The background counting rate was less than five percent of the source counting rate at the lowest energy measured. At this energy the background was twenty counts per minute per channel and it decreased rapidly to about one count per minute per channel near the end point. The window widths for the ten-channel analyzer were 2%, and the resolution for this run was 12.9% for the Cs^{137} line.

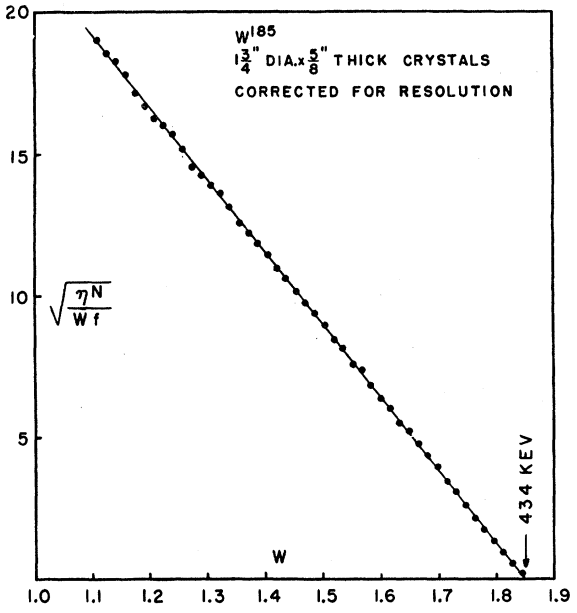

FIG. 5. W^{185} Fermi-Kurie plot.

The second run on Cl^{36} was made with a 20-$\mu g/cm^2$ source. At least 10^4 counts were obtained for each point on the spectrum below 500 kev and at least 10^3 counts were obtained for each point below 680 kev. New phototubes resulted in an improvement of the resolution to 11.4% for the Cs^{137} line. The window widths for the ten-channel analyzer were 2% and the data from this run are plotted in Fig. 6.

The third run on Cl^{36} was made with a 19-$\mu g/cm^2$ source and was obtained in essentially the same manner as the previous run. The resolution for the Cs^{137} line was 11.7% and the total time between the initial and the final calibration was about six hours.

The resolution corrections of Palmer and Laslett[12] were applied to the data from each of the three runs. These corrections were 2% or less at each point except

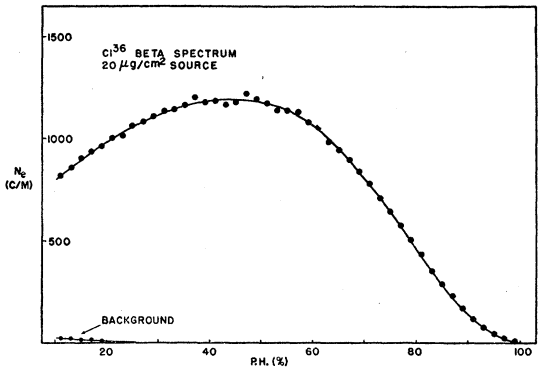

FIG. 6. Cl^{36} beta spectrum from 20-$\mu g/cm^2$ source.

for the five points nearest the end point which were corrected by the "end-point correction."[12] A conventional F-K plot of the data from the 20 $\mu g/cm^2$ source is shown by the upper curve in Fig. 7, and the deviation from an allowed shape is obvious. The experimental data extends down to 89 kev.

In order to compare the present measurements with those of previous investigators,[1,2] and analysis of the data was made using the unique twice forbidden shape factor, although this shape factor is applicable only for a spin change of 3. This analysis affords a convenient method of comparing the data since this shape factor has a unique energy dependence and had been used by the previous investigators to analyze their data. This shape factor was applied to all three of the runs made in the present investigation and in each case it failed to linearize the F-K plot. The lower curve in Fig. 6 shows the F-K plot of the data from the 20-$\mu g/cm^2$ source with the unique twice forbidden shape factor included. The deviation from linearity is in good agreement with the results of Fulbright and Milton whose data, however, extended down only to about 180 kev.

THEORETICAL INTERPRETATION

The beta spectrum for a twice forbidden transition is described by an equation which gives the number of

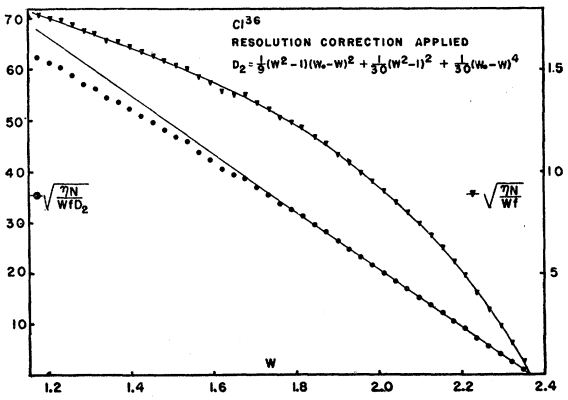

FIG. 7. Cl^{36} Fermi-Kurie plot—conventional and with unique twice forbidden shape factor.

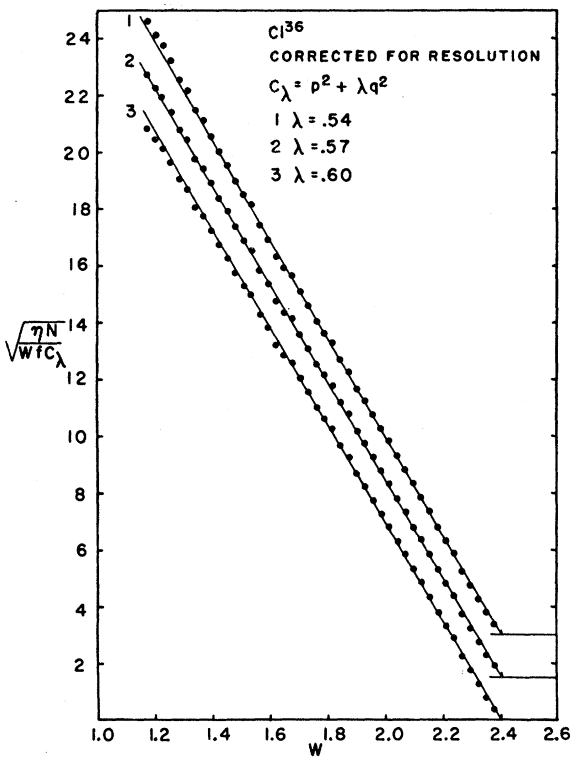

FIG. 8. Cl^{36} Fermi-Kurie plots with C_λ included.

electrons $N(W)$ emitted in the energy range between W and $W+dW$, as

$$N(W)dW=(g^2/2\pi^3)F(Z,W)\eta W(W_0-W)^2S_2(W), \quad (1)$$

where the energy W and momentum η of the electron are in relativistic units. W_0 is the end-point energy of the spectrum, g is the Fermi coupling constant, and $F(Z,W)$ is the Coulomb factor. It is the "shape factor," $S_2(W)$, that is of particular interest here. It depends parametrically on the nuclear moments responsible for the β radiation. Determination of the parameters through fitting $S_2(W)$ to the experimental spectrum should, in principle, serve to measure ratios of nuclear β moments of the Cl^{36} transition.

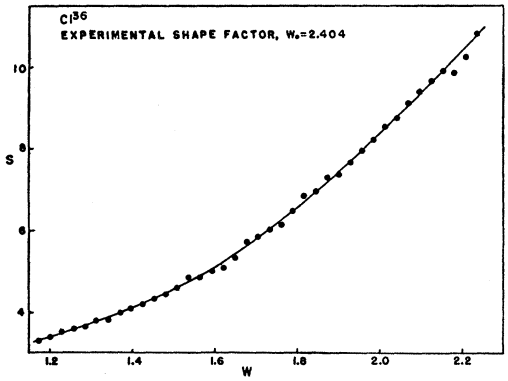

FIG. 9. Cl^{36} experimental shape factor.

The "exact" theoretical shape factor, $S_2(W)$, as presented by Konopinski,[13] was used here. It was found convenient to replace the parameters ξ_2, η_2 in Konopinski's notation with

$$\xi'=\frac{C_S}{C_T}\xi_2=2i\frac{C_S}{C_T}\frac{R_{ij}}{T_{ij}}, \quad \eta'=\frac{\alpha Z}{2R}\eta_2=\frac{A_{ij}}{T_{ij}}. \quad (2)$$

Here, C_S and C_T are the coupling strengths for the scalar and tensor β interactions. They are known to be of about the same absolute magnitude. R_{ij} is, in conventional notation, a nuclear β moment through which the scalar interaction contributes. Similarly, the tensor interaction contributes through both the nuclear matrix elements T_{ij} and A_{ij}.

An experimental shape factor is obtained as

$$S_2(\text{exp})\sim N(W)/\eta W(W_0-W)^2F(Z,W) \quad (3)$$

by putting the experimental values of $N(W)$ into (1). Clearly, S_2(exp) becomes very sensitive to the value

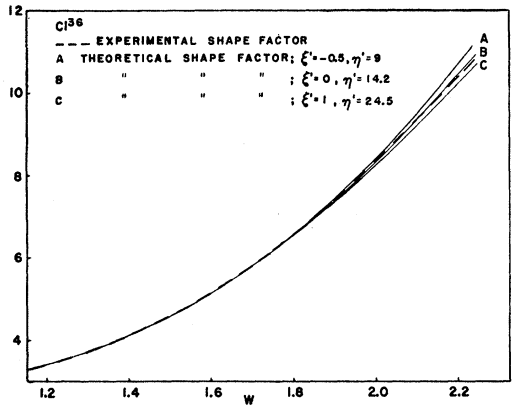

FIG. 10. Comparison of exact shape factors for best fit to data.

adopted for the end-point energy, W_0, for energies W near W_0. It should be noted, however, that any uncertainties in W_0 arising from calibration will affect W_0-W negligibly. Hence, this contributes very little to the uncertainty in S_2(exp).

To obtain a value for W_0, a preliminary fitting with a low-Z approximation to the theoretical shape factor should be sufficient (since Coulomb effects are least important at high energies):

$$S_2(\alpha Z\ll 1)\sim C_\lambda=\eta^2+\lambda q^2. \quad (4)$$

Here, η is the electron momentum, as before, and $q=W_0-W$ is the neutrino momentum in units mc. Only one parameter, λ, remains in this approximation and its relation to η' and ξ' of (2) is

$$\lambda=4\frac{[(\alpha Z/2R)(1+\xi')-\eta']^2}{[(\alpha Z/2R)(1+\xi')-2\eta']^2}. \quad (5)$$

[13] E. J. Konopinski, *Beta- and Gamma-Ray Spectroscopy*, edited by K. Siegbahn (Interscience Publishers, Inc., New York, 1955), Chap. 10.

This was used as a variable parameter in fitting C_λ to the experimental data. As expected, the fitting depended only weakly on the choice of W_0. The conventional method of "linearizing" the F-K plot was used, i.e.,

$$(N/\eta WFC_\lambda)^{\frac{1}{2}} \tag{6}$$

which is theoretically $\sim(W_0-W)$, was plotted against W, for various values of λ. The best fit, as shown in Fig. 8, was found for $\lambda=0.57$. This gives an end-point energy of 717 kev. Figure 8 also shows the deviation from linearity when $\lambda=0.54$ and $\lambda=0.60$ are used. The straight lines were determined through a least squares fitting of all points having $W>1.70$, excluding the five points nearest W_0. For an end-point energy of 717 kev, the experimental shape factor shown in Fig. 9 is obtained.

The "exact" shape factor $S_2(w)$ depends on the two parameters ξ', η', of (2) instead of the single one, λ, which remains in the low-Z approximation. In fitting to the experimental data, $S_2(\text{exp})$, values of ξ' from -1 to $+50$ were tried. For each trial, η' was determined to

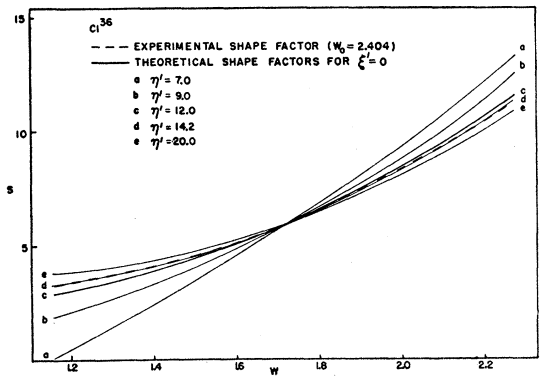

FIG. 11. Comparison of exact shape factors for $\xi'=0$.

give the best fit. The best agreement between $S_2(\text{exp})$ and the theoretical shape factor was found for $\xi'=0$ and $\eta'=14.2$. This fit is shown in Fig. 10, together with the best fits for $\xi'=-\frac{1}{2}$ and $\xi'=+1$. Figure 11 shows the theoretical curves for $\xi'=0$ and various values of η'.

It is thus found that the best fit with the data ($\xi'=0$) is obtained from the Tensor coupling alone [see (2)]. The conclusion from this is that the scalar-interaction moment, R_{ij}, must be small compared to the tensor-interaction moment, T_{ij}.

However, caution is necessary in accepting this conclusion. Large uncertainties are caused by the extreme sensitivity, pointed out above, of $S_2(\text{exp})$ in (3), to the exact value of W_0. To investigate this, $S_2(\text{exp})$ was also evaluated for two end-point energies differing from 717 kev by $\pm\frac{1}{2}\%$. The experimental shape factors which result are shown by the curves A and B in Fig. 12. Taking these as the limits on the uncertainty in $S_2(\text{exp})$, the following limits on ξ' and η' are obtained:

$$-0.7<\xi'<2.0 \quad \text{for} \quad 6.5<\eta'<35. \tag{7}$$

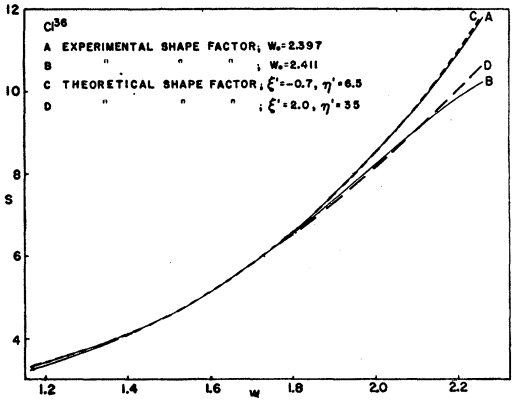

FIG. 12. Exact shape factors for limits of ξ' and η'.

The theoretical shapes factors for these limits are shown by the curves C and D in Fig. 12.

To compare the three runs on Cl^{36}, the exact theoretical shape factor with $\xi'=0$ and $\eta'=14.2$, which was obtained for the spectrum from the 20-μg/cm^2 source, was also used to analyze the spectra obtained from the other two sources. The F-K plots, with this shape factor included, are shown in Fig. 13. No variations among the F-K plots due to source thickness effects are evident, and the average end-point energy is 714 ± 4 kev.

In previously published work on the analysis of the Cl^{36} spectrum, no attempt was made to include the scalar coupling, as here; the tensor interaction alone was considered. However, our result that the best fit is obtained without scalar coupling makes a direct comparison with the old results possible. Moreover, the old analyses were confined to a low-Z approximation, comparable to (4); this procedure should yield a value for the single parameter λ, irrespective of the assumptions about the coupling. The latter pertains only to the relation (5) of λ to ξ' and η'.

Wu and Feldman quote their finding as $\eta'=4.2$ and Fulbright and Milton as $\eta'=5.1$. Both automatically presumed $\xi'=0$ by using a purely tensor coupling. These findings appear to be in thorough disagreement

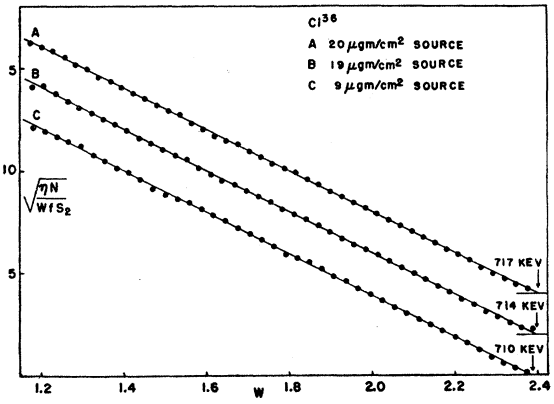

FIG. 13. Fermi-Kurie plots with S_2 included for three runs on Cl^{36}.

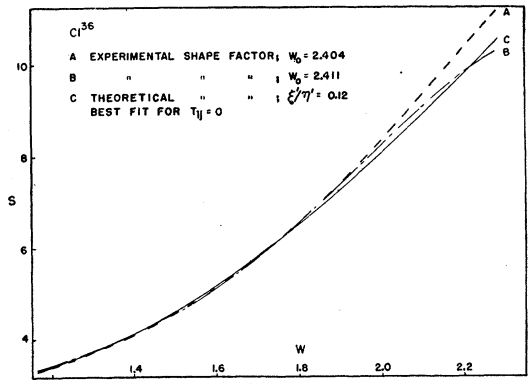

FIG. 14. Best fit of S_2 to data for $T_{ij}=0$.

with the present conclusion that $\xi'=0$ and $\eta'=14.2$. Only by straining the limits on the uncertainty, as in (7), can we approach as low a value as 6.5.

The resolution of the disagreement rests on the following. The analyses using the low-Z approximation are only capable of determining the parameter λ of (4), and (5). In our own preliminary fitting, we found $\lambda=0.57\pm0.03$, as quoted above. If we now use our exact fitting results, $\xi'=0$ and $\eta'=14.2$, in (5), we find $\lambda=0.60$, showing that the low-Z approximation is a good one.

It appears, therefore, that the previous workers happened upon the wrong root, η', of the two possible roots of the quadratic (5) for $\eta'(\lambda)$. The more exact analysis shows that the correct root, η', is 3 to 4 times as large as that quoted by the previous workers. This was checked by actual trial of the low root in the exact shape factor. We also found that, if we followed the same approximate procedure as did the previous workers, we obtain equally good agreements with $\eta'\approx13.5$ and $\eta'\approx4.5$. The more exact work shows that the second of these two values is spurious.

Our conclusion that the matrix element R_{ij} is negligible compared to T_{ij}, for Cl^{36}, disagrees with the predictions based on the shell model, by Peaslee[14] and Fowler.[15] These investigators report instead that $T_{ij}=0$ and that a finite R_{ij} is to be expected. The expectation is based on the presumption that, in the Cl^{36} transition, a $d_{\frac{3}{2}}$ neutron is transformed into a $d_{\frac{3}{2}}$ proton. The prediction is unchanged[16] as long as only $d_{\frac{3}{2}}$ particles are admitted into the open shell of Cl^{36}. The inconsistency of the present measurements with the theoretical prediction $T_{ij}=0$ was checked directly. Figure 14 shows the results. After $T_{ij}=0$ is put into the exact theoretical shape factor, it retains only one parameter $\theta=\xi'/\eta'$. Values of θ from -0.1 to $+0.5$ were tried and Fig. 14 shows that the best fit to this family of theoretical curves is obtained for $\theta=0.12$. Even this, however, is outside the uncertainty in the experimental shape factor. Moreover, from Eq. (5), $\theta=0.12$ leads to $\lambda=0.29$ when $T_{ij}=0$, and this is inconsistent with $\lambda=0.57$, which was found using λ as a variable parameter in (4).

On even less secure grounds that those of the shell model, Fowler also predicts $A_{ij}=0$ for Cl^{36}. In effect, he would have the Cl^{36} transition be generated solely by the scalar coupling; yielding $\lambda=4$. This is entirely inconsistent with all the analyses of the experimental spectrum.

ACKNOWLEDGMENTS

The authors are indebted to Professor E. J. Konopinski for his invaluable assistance with the theoretical aspects of this problem.

[14] D. C. Peaslee, Phys. Rev. **91**, 1447 (1953).
[15] G. N. Fowler, Proc. Phys. Soc. (London) **A67**, 1005 (1954).
[16] We are indebted to Professor E. J. Konopinski and Mr. N. D. Newby, Jr., for a clarification of this point.